Available online at www.sciencedirect.com
ScienceDirect
Ceramics International 37 (2011) 327–331
CERAMICS INTERNATIONAL
www.elsevier.com/locate/ceramint

Photocatalytic properties of TiO_2 sol–gel modified nanocomposite films

Akbar Eshaghi [a,b,*], Reza Mozaffarinia [b], Mahmoud Pakshir [a], Ameneh Eshaghi [c]

[a] Department of Materials Science and Engineering, Faculty of Engineering, Shiraz University, Shiraz, Iran
[b] Faculty of Materials Science and Engineering, Maleke Ashtar University of Technology, Esfahan, Iran
[c] IslamicAzad University, Sari, Iran

Received 28 May 2010; received in revised form 6 July 2010; accepted 28 August 2010
Available online 24 September 2010

Abstract

TiO_2 nanocomposite films with different concentrations of TiO_2 MT-150A nanoparticles were immobilized on glass substrates using a dip coating process. The crystalline structure and surface chemical state of nanocomposite film properties were examined by X-ray diffraction (XRD) and X-ray photoelectron spectroscopy (XPS), respectively. The specific surface area and morphology of TiO_2 MT-150A nanoparticles were evaluated by the BET method and Field Emission Scanning Electron Microscopy (FE-SEM). The photocatalytic activities of films were evaluated by the methyl orange decoloring rate. XPS measurements showed that the oxygen amount (%) was related to the film composition. The composite film with 10 g/L MT-150A loading yielded the highest amount of surface oxygen (26.82%) and TiO_2 rutile showed the lowest amount of surface oxygen (13.67%) in the form of surface hydroxyl groups. The remaining oxygen was identified as lattice oxygen. In addition, the nanocomposite film with 10 g/L MT-150A loading yielded the highest photocatalytic activity.

Keywords: A. Sol–gel processes; B. Nanocomposites; D. TiO_2

1. Introduction

TiO_2 is of interest as a photocatalyst for the degradation of several environmental contaminants [1–5]. Many organic compounds can be decomposed in aqueous solution in the presence of TiO_2 under UV light irradiation .For example, azo-dyes like alizarin S, crocein orange G, methyl red, congo red and methylene blue have been completely mineralized with TiO_2/UV in aqueous suspensions [6]. In recent years, titanium dioxide (TiO_2) based nanocomposite have attracted much attention in photocatalytic applications [7].

Sol–gel processing is one of the most common methods to produce TiO_2 nanocomposites. This process involves the hydrolysis and polycondensation of a precursor (e.g. metal alkoxide) and subsequent formation of the gel, which results in a crystalline network structure after heat treatment. The sol–gel technique provides many advantages over conventional methods such as low processing temperature, homogeneity, possibility of coating on large area substrates, and cost effective [8,9]. Furthermore, incorporating TiO_2 nanoparticles as nanofillers into titanium alkoxide solution to form nanocomposite film has been proved to be a promising technique to prepare TiO_2 coatings for photocatalytic applications such as water and air purification as well as dye sensitized solar cells [10–14]. The relationship of TiO_2 particles with TiO_2 formed from a sol precursor via hydrolysis/condensation and crystallization process was in fact a host–guest relationship in the composite films. The advantage of using this technique for the preparation of TiO_2 films is that the high purity commercial TiO_2 nanoparticles can be well glued by the presence of sol–gel derived TiO_2 matrix [12,15,16].

In this study, we employed commercial titania nanoparticles, MT-150A, and incorporated them into a TiO_2 matrix prepared from a titanium alkoxide precursor sol. Titania powder modified films were produced using a dip coating sol–gel process. Then, hydrophilicity, photocatalytic and self cleaning properties of nanocomposite films were investigated.

2. Experimental

2.1. Nanocomposite film preparation

First, a TiO_2 precursor sol was prepared as following: acetyl acetone (0.57 mol) and titanium tetraisopropoxide (1 mol) were

* Corresponding author at: Department of Materials Science and Engineering, Faculty of Engineering, Shiraz University, Shiraz, Iran.
Tel.: +98 0312 5225041; fax: +98 0312 5228530.

0272-8842/$36.00
doi:10.1016/j.ceramint.2010.09.008

dissolved in order in 1-butanol (12 mol) to form solution A; a mixture of deionized water (2 mol) and 1-butanol (8 mol) was obtained as solution B. Solution B was then added to solution A dropwise under stirring. The resulting sol was then aged for 12 h. Acetyl acetone was added to slow the speed of hydrolysis and condensation reactions and form a stable sol.

For the synthesis of titania nanoparticles modified films, TiO_2 MT-150A, TAYCA, nanoparticles with 0, 10, 30, 50 and 70 g/L were added slowly in TiO_2 sol under vigorous stirring to avoid the formation of larger titania agglomerates in the sol. To obtain a homogeneous distribution, the solution was stirred at room temperature for 12 h. A white and viscous solution was obtained. The films were obtained by a dip coating method and withdrawn at the speed of 5.33 cm/min. The films were air dried for 2 h, and then were heat-treated at 500 °C for 1 h in air (heating rate 10°C/min). This procedure was carried out five times. Before coating, glass substrates were ultrasonically cleaned in acetone and ethanol for 15 and 20 min, respectively.

To make photocatalytic comparison, TiO_2 MT-150A colloidal sol was prepared by ball milling: the TiO_2 paste solution was prepared by dissolving of TiO_2 MT-150A powder (0.5 g) in water (4.5 mL) and surfactant (POIZ, 50 mg). To prepare paste solution and to avoid the formation of larger titania agglomerates in the TiO_2 sol, ZrO_2 balls (5 g) were introduced in the solution which was milled for 3 h (500 rpm). After that, ZrO_2 balls were removed from the solution and the volume of paste solution was increased to 100 mL using deionized water. Then, the film was deposited on the glass substrate according to the method mentioned above.

2.2. Film characterization

The crystal phase composition of titania powder modified films and their TiO_2 matrix (without MT-150A) were determined by XRD (Philips powder diffractometer, Cu Kα radiation). The surface chemical state of the films was analyzed by X-ray photoelectron spectroscopy (XPS, JEOL) using Mg Kα source (1253.6 eV). The X-ray source was operated at 10 kV for a current of 10 mA. Spectra were calibrated with respect to the C1s peak at 284.6 eV [17].

The specific surface area and morphology of the TiO_2 MT-150A nanoparticles were evaluated by the BET method and Field Emission Scanning Electron Microscopy (FE-SEM; JEOL).

The hydrophilicity of the films was evaluated by measuring the contact angle of a water droplet on the film surfaces. A droplet was injected on to the surface using a 1 μL micro-injector (Kyowa Interface Science, Drop Master 500). The water contact angle was averaged from five measurements. UV–Vis was irradiated to the surface of the samples by Xe lamp (power 300 W, wavelength 300–500 nm). In the part of water contact angle measurements, samples were stored in a drying oven at 100 °C for at least 12 h before use. In addition, the hydrophilic–hydrophobic conversion of films after storage in a dark place was investigated.

The photocatalytic activities of films under UV irradiation were evaluated by the decoloring rate of methyl orange

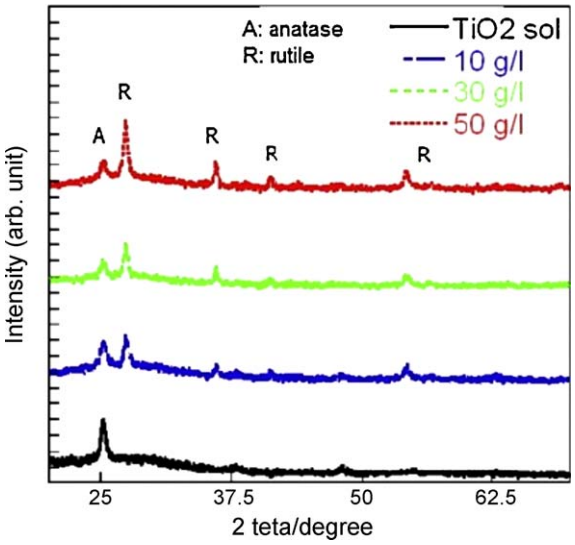

Fig. 1. X-ray diffraction patterns of film samples.

($C_{14}H_{14}N_3SO_3Na$). Methyl orange was also used as a model organic compound to measure the photoreactivity in other studies [18,19].

One sample of film (surface area 6 cm^2) was horizontally placed at the bottom of the testing cell containing 25 mL (2×10^{-5} M) methyl orange solution. The solution was irradiated with 300 W ultraviolet light. The distance between the sample and irradiation source was 8 cm. After irradiation, the light absorbance of methyl orange solution was measured using a UV–vis spectrophotometer at 464 nm, which is the maximum absorption of methyl orange [20]. Then, the decoloring rate of methyl orange, was used to quantify the photocatalytic activities of thin films, and calculated using following equation: [21]

$$\eta = \frac{A_0 - A}{A_0} \times 100 \quad (1)$$

where A_0 is the light absorbance of methyl orange before the irradiation (absorption equilibrium in the dark place for 30 min) and A is the light absorbance of methyl orange after the irradiation (see Fig. 1).

3. Results and discussion

3.1. Crystalline structure

The XRD patterns of the nanocomposite film samples are shown in Fig. 2.

From the XRD pattern, the percentage of anatase phase can be calculated using Eq. (2):

$$\%\ \text{of anatase phase} = \frac{100}{1 + (I_R/0.79I_A)} \quad (2)$$

where I_A and I_R are the strongest intensities of anatase phase along the (1 0 1) plane and rutile phase along (1 1 0), [21]. The

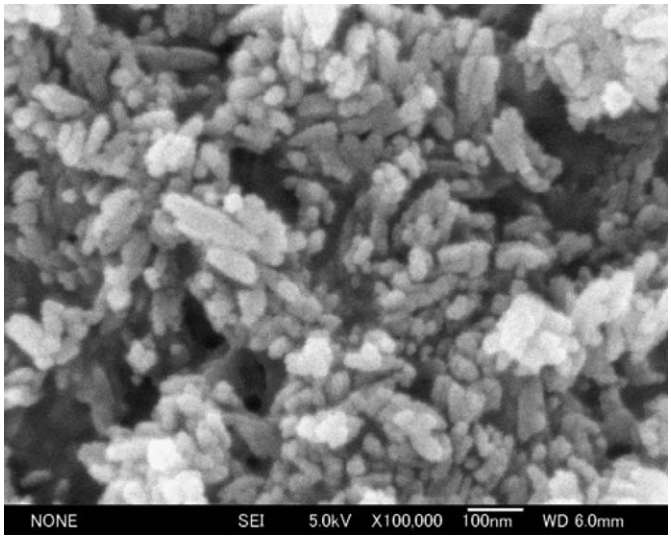

Fig. 2. FE-SEM image of TiO_2 MT-150A nanoparticles.

Table 1
Effect of titania loading on crystal percent and crystal size of nanocomposite films.

Sample	%anatase	%rutile	Anatase size (nm)
TiO_2 matrix	100	0	16
10 g/L	43	57	13.4
30 g/L	32	68	12.6
50 g/L	27	73	11.5

percentages of anatase phase in TiO2 matrix and composite sol–gel modified TiO_2 films are summarized in Table 1.

The average crystallite size of the anatase phase of films was calculated from the Scherrer equation [22], using the (1 0 1) peak:

$$t = \frac{K\lambda}{\beta \cos\theta} \quad (3)$$

where t is the grain size, K is a constant (0.9), λ is the wavelength of X-ray (Cu Kα), β is the half-peak width, and θ is the diffraction angle in degree.

In the nanocomposite film samples, with the addition of MT-150A nanoparticles, the XRD peak gradually becomes broader. It means that the crystalline size of TiO_2 becomes smaller with the addition of additives. In the composite film, the size of TiO_2 crystallites was smaller than in the pure TiO_2 (Table 1). Moreover, Yu et al. [23] indicated that increase of additives to titania hindered the crystal growth of TiO_2.

3.2. TiO_2 MT-150A nanoparticles

The specific surface area of the TiO_2 MT-150A nanoparticles, evaluated by the BET method, was 101.84 m^2/g. Fig. 3 shows a FE-SEM image of TiO_2 MT-150A particles. It can be derived that the average size of particles is in the range of 10–20 nm.

3.3. XPS studies

Fig. 3 shows XPS scan spectra for 10 g/L nanocomposite film. The surface chemical state of the films was analyzed by high resolution XPS. Fig. 3b shows the Ti 2p XPS spectra of the 10 g/L composite film. The binding energies of Ti 2p3/2 and Ti 2p1/2 were observed at 458.2 and 463.9 eV, respectively, with a separation of 5.7 eV between the two peaks. This is a typical characteristic of the Ti^{4+} state in TiO_2. In addition, the Ti 2p XPS peak is sharp and strong, indicating that the Ti element exists mainly as the chemical state of Ti^{4+} in the films [24,25]. Therefore, an XPS spectrum confirmed that the film contains only titania.

3.4. Photocatalytic activity

The photocatalytic activities of films were characterized by the degradation of methyl orange. The methyl orange degradation rate after 3 h irradiation in the presence of nanocomposite films is shown in Fig. 4, showing 10 g/L nanocomposite film to have the highest photocatalytic activity. The results reveal that the photocatalytic performance of TiO_2 can be improved by the formation of nanocomposite films.

TiO_2 is a semiconductor with band gap energy of 3.2 eV. When titanium oxide is irradiated with UV light ($\lambda < 380$ nm),

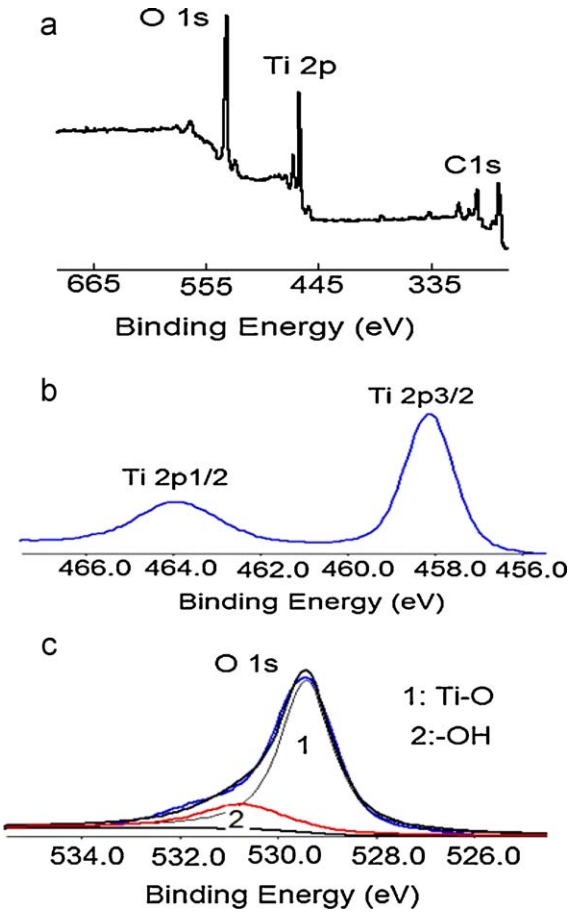

Fig. 3. XPS spectra of 10 g/L nanocomposite film (a) wide scan and (b) high-resolution spectra of Ti 2p and (c) O1s.

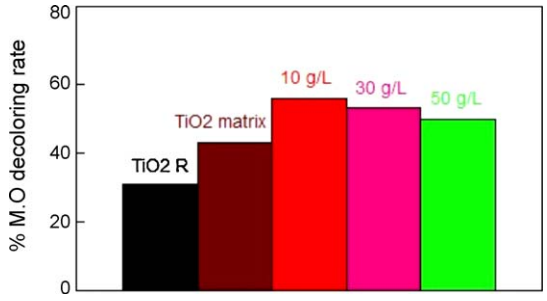

Fig. 4. Methyl orange decoloring rate.

the electrons and holes are produced in conduction band and valence band, respectively as for:

$$TiO_2 + h\upsilon \rightarrow TiO_2\ (e^-_{CB} + h^+_{VB})$$
(Photo generation of electrons and holes) (4)

These photo electron–hole pairs have an oxidizing potential which is sufficient to oxidize most pollutants present in aqueous systems. The photogenerated electrons react with molecular oxygen (O_2) to produce superoxide radical anions (O_2^-), and photogenerated holes react with water to produce hydroxyl radicals. These highly reactive species are able to decompose a variety of organic compounds [26,27].

Based on [28], the photodegradation reaction of methyl orange (MO) on the nanocomposite TiO_2 film surface can be written as follow:

$$MO + TiO_2 \xrightarrow{h\upsilon} CO_2 + NO_3^- + SO_4^{2-} \quad (12)$$

Wholly, the photoactivity of TiO_2 depends on several parameters such as surface hydroxyl group density, crystalline structure, recombination rate of electron–hole pairs. Crystalline structure has a significant effect on the photocatalytic efficiency of TiO_2. These results confirmed the effect of crystalline phase on the photoreactivity of TiO_2. Many researchers confirmed that the anatase phase has higher photoreactivity than the rutile phase [29]. This difference can be related to oxidation and reduction potential of photo generated holes and electrons in the conduction and valance bands in the anatase and rutile phase. In addition, it is believed that a combination of anatase and rutile has a higher photoreactivity than anatase or rutile alone [30–32]. Therefore, nanocomposite film with a higher fraction of anatase phase has higher photoactivity.

In addition, it is well accepted that hydroxyl groups have a significant effect on the photoreactivity of TiO_2. XPS is one of the most useful methods to measure hydroxyl group content on the film surfaces. The O 1s XPS spectrum of 10 g/L nanocomposite film is displayed in Fig. 3c. In the literature, the O 1s peak is often believed to be composed of 3–5 different oxygen species, such as Ti–O bonds in TiO_2 and Ti_2O_3, hydroxyl groups, C–O bonds, and adsorbed H_2O [33].

To get reliable data and statistics, the O 1s peak will be modeled with two pseudo-Voigt functions with peak 1 in Fig. 3c, related to lattice oxygen in TiO_2 and with peak 2 corresponding to surface oxygen, in the form of OH in Ti–OH (surface hydroxyl group). The hydroxyl content (%) is the ratio of the area of peak 2 to the total area of the two O 1s peaks. In Table 2, the fit parameters for the O 1s peak are shown for MT-150A, TiO_2 matrix and 10 g/L nanocomposite film. It is the largest for the 10 g/L nanocomposite film and is the smallest for MT-150A. It is noted that the hydroxyl content in the nanocomposite film is higher than that in TiO_2, indicating the amount of the hydroxyl group to result from the chemisorption of water molecules on the TiO_2 surface enhanced by the formation of nanocomposite film. Although some water is easily adsorbed on the surface of TiO_2 films during the deposition process, the physically absorbed water on TiO_2 is easily desorbed under the ultrahigh vacuum condition of the XPS system. Therefore, the XPS spectrum only shows chemisorbed water. It means that the hydroxyl on the surface can be attributed to the Ti–OH group. Hydroxyl groups are important factors in the TiO_2 because not only they can reduce the recombination of electron–hole pairs but also they have a strong photo-oxidation capability which can improve the photocatalytic activity of the films [34].

Table 2
Fit parameters for the O 1s peak.

	MT-150A	TiO_2 matrix	10 g/L
Area 1	3903.192	3390.751	2972.1
Area 2	618.1	690.85	1089.35
E_{K1} (eV)	528.7	529.68	529.50
Hydroxyl content (%)	13.67	16.9	26.82

Methyl orange is attacked by hydroxyl radicals and generates inorganic radicals or some other intermediates. Eventually methyl orange and intermediate compounds are oxidized into CO_2, SO_4^{2-}, and NO^{3-}.

The 10 g/L nanocomposite film shows the highest photoactivity due to the highest surface hydroxyl groups and the highest fraction of the anatase phase.

4. Conclusions

MT-150A loading has been shown to have a significant effect on structural properties and photocatalytic activity. The photocatalytic activity can be improved significantly by the formation of nanocomposite films including MT-150A nanoparticles in TiO_2 sol–gel derived matrix. This can be explained by the change in film structural properties by: (i) a change in the crystalline phases (anatase and rutile), (ii) a decrease in the crystallite size, i.e. increases in the amount of surface active area and (iii) an increase in the hydroxyl group density. It is concluded that the crystal structure and hydroxyl group density of the TiO_2 nanocomposite films are two critical factors for photocatalytic activity. Therefore, TiO_2 nanocomposite sol–gel derived film would possibly be more useful than pure TiO_2 film in exhibiting photoreactivity for practical applications such as the self cleaning effect in building applications.

Acknowledgments

We are grateful to Ministry of Research, Science and Technology of Iran to support this work. We thank Prof. Ohtani for using XPS.

References

[1] M.H. Chan, W.Y. Ho, D.Y. Wang, F.H. Lu, Characterization of Cr-doped TiO_2 thin films prepared by cathodic arc plasma deposition, Surf. Coat. Technol. 202 (2007) 962–966.
[2] Y. Zhang, J. Wan, Y. Ke, A novel approach of preparing TiO_2 films at low temperature and its application in photocatalytic degradation of methyl orange, J. Hazard. Mater. 177 (2010) 750–754.
[3] Z.Z. Deng, F. Chen, J. Zng, H. Chen, M. Anpo, J. Huang, L. Zhang, Hydrothermal doping method for preparation of Cr^{3+}–TiO_2 photocatalysts with concentration gradient distribution of Cr^{3+}, Appl. Catal. B: Environ. 62 (2006) 329–335.
[4] D. Mardare, D. Luca, C.M. Teodorescu, D. Macovei, On the hydrophilicity of nitrogen-doped TiO_2 thin films, Surf. Sci. 601 (2007) 4515–4520.
[5] C.C. Tsai, H. Teng, Chromium-doped titanium dioxide thin-film photoanodes in visible-light-induced water cleavage, Appl. Surf. Sci. 254 (2008) 4912–4918.
[6] J. Tang, Z. Zou, J. Yin, J. Ye, Photocatalytic degradation of methylene blue on $CaIn_2O_4$ under visible light irradiation, Chem. Phys. Lett. 382 (2003) 175–179.
[7] H. Narayan, H. Alemu, L. Macheli, M. Sekota, M. Thakurdesa, T.K.G. Rao, Role of particle size in visible light photocatalysis of Congo Red using $TiO_2{\cdot}[ZnFe_2O_4]_x$, Bull. Mater. Sci. 32 (2009) 499–506.
[8] M. Keshmiri, M. Mohseni, T. Troczynski, Development of novel TiO_2 sol–gel-derived composite and its photocatalytic activities for trichloroethylene oxidation, Appl. Catal. B: Environ. Appl. Catal. B: Environ. 53 (2004) 209–219.
[9] T. Olding, M. Sayer, D. Barrow, Ceramic sol–gel composite coatings for electrical insulation, Thin Solid Films 398–399 (2001) 581–586.
[10] G. Balasubramanian, D.D. Dionysiou, M.T. Suidan, V. Subramanian, I. Baudin, J.M. Laine, Titania powder modified sol–gel process for photocatalytic applications, J. Mater. Sci. 38 (2003) 823–831.
[11] G. Balasubramanian, D.D. Dionysiou, M.T. Suidan, I. Baudin, J.M. Laine, Evaluating the activities of immobilized TiO_2 powder films for the photocatalytic degradation of organic contaminants in water, Appl. Catal. B: Environ. 47 (2004) 73–84.
[12] Y. Chen, D.D. Dionysiou, TiO_2 photocatalytic films on stainless steel: the role of Degussa P-25 in modified sol–gel methods, Appl. Catal. B: Environ. 62 (2006) 255–264.
[13] Y.J. Chen, D.D. Dionysiou, A comparative study on physicochemical properties and photocatalytic behavior of macroporous TiO_2-P25 composite films and macroporous TiO_2 films coated on stainless steel substrate, Appl. Catal. A: Gen. 317 (2007) 129–137.
[14] Y.J. Chen, D.D. Dionysiou, Bimodal mesoporous TiO_2-P25 composite thick films with high photocatalytic activity and improved structural integrity, Appl. Catal. B: Environ. 80 (2008) 147–155.
[15] W. Que, Q.Y. Zhang, Y.C. Chan, C.H. Kam, Sol–gel derived hard optical coatings via organic/inorganic composites, Compos. Sci. Technol. 63 (2003) 347–351.
[16] Y. Chen, E. Stathatos, D.D. Dionysiou, Sol–gel modified TiO_2 powder films for high performance dye-sensitized solar cells, J. Photochem. Photobiol. A: Chem. 203 (2009) 192–198.
[17] S.D. Sharma, D. Singh, K.K. Saini, C. Kant, V. Sharma, S.C. Jain, C.P. Sharma, Sol–gel-derived super-hydrophilic nickel doped TiO_2 film as active photo-catalyst, Appl. Catal. A: Gen. 314 (2006) 40–46.
[18] L. Chen, J. Tian, H. Qiu, Y. Yin, X. Wang, J. Dai, P. Wu, A. Wang, L. Chu, Preparation of TiO_2 nanofilm via sol–gel process and its photocatalytic activity for degradation of methyl orange, Ceram. Int. 35 (2009) 3275–3280.
[19] J. Wang, B. Guo, X. Zhang, J. Han, J. Wu, Sonocatalytic degradation of methyl orange in the presence of TiO_2 catalysts and catalytic activity comparison of rutile and anatase, Ultrason. Sonochem. 12 (2005) 331–337.
[20] H. Tian, J. Ma, K. Li, J. Li, Hydrothermal synthesis of S-doped TiO_2 nanoparticles and their photocatalytic ability for degradation of methyl orange, Ceram. Int. 35 (2009) 1289–1292.
[21] J. Chen, M. Yao, X. Wang, Investigation of transition metal ion doping behaviors on TiO_2 nanoparticles, J. Nanopart. Res. 10 (2008) 163–171.
[22] P. Klug, L.E. Alexander, X-ray Diffraction Procedures, Wiley, New York, 1974.
[23] J. Yu, X. Zhao, J. Yu, G. Zhong, The grain size and surface hydroxyl content of super-hydrophilic TiO_2/SiO_2 composite nanometer thin films, J. Mater. Sci. Lett. 20 (2001) 1745–1748.
[24] L. Ge, M. Xu, H. Fang, M. Sun, Preparation of TiO_2 thin films from autoclaved sol containing needle-like anatase crystals, Appl. Surf. Sci. 253 (2006) 720–725.
[25] F. Mei, C. Liu, L. Zhang, F. Ren, L. Zhou, W.K. Zhao, Y.L. Fang, Microstructural study of binary TiO_2:SiO_2 nanocrystalline thin films, J. Cryst. Growth 292 (2006) 87–91.
[26] K.M. Parida, N. Sahu, Visible light induced photocatalytic activity of rare earth titania nanocomposites, J. Mol. Catal. A: Chem. 287 (2008) 151–158.
[27] J.O. Carneiro, V. Teixeira, A. Portinha, A. Magalhaes, P. Coutinbo, C. Tavares, Iron-doped photocatalytic TiO_2 sputtered coatings on plastics for self-cleaning applications, J. Mater. Sci. Eng. B 138 (2007) 144–150.
[28] A. Houas, H. Lachheb, M. Ksibi, E. Elaloui, C. Guillard, J.M. Herrmann, Photocatalytic degradation pathway of methylene blue in water, Appl. Catal. B: Environ. 31 (2001) 145–157.
[29] S. Kim, S.H. Ehrman, Photocatalytic activity of a surface-modified anatase and rutile titania nanoparticle mixture, J. Colloid Interface Sci. 338 (2009) 304–307.
[30] X.F. Zhou, D.B. Chu, S.W. Wang, C.J. Lin, Z.Q. Tian, New route to prepare nanocrystalline TiO_2 and its reaction mechanism, Mater. Res. Bull. 37 (2002) 1851–1857.
[31] T. Ohno, K. Tokieda, S. Higashida, M. Matsumura, Synergism between rutile and anatase TiO_2 particles in photocatalytic oxidation of naphthalene, Appl. Catal. A: Gen. 244 (2003) 383–391.
[32] S. Bakardjieva, J. Subrt, V. Stengl, M.J. Dianez, M.J. Sayagues, Photoactivity of anatase–rutile TiO_2 nanocrystalline mixtures obtained by heat treatment of homogeneously precipitated anatase, Appl. Catal. B: Environ. 58 (2005) 193–202.
[33] H. Jensen, A. Solovieva, Z. Lib, E.G. Sogaard, XPS and FTIR investigation of the surface properties of different prepared titania nano-powders, Appl. Surf. Sci. 246 (2005) 239–249.
[34] K. Guan, Y. Yin, Effect of rare earth addition on super-hydrophilic property of TiO_2/SiO_2 composite film, Mater. Chem. Phys. 92 (2005) 10–15.